Heliyon 6 (2020) e04028

Contents lists available at ScienceDirect

Heliyon

journal homepage: www.cell.com/heliyon

Research article

Role of FOXM1 in vascular smooth muscle cell survival and neointima formation following vascular injury

Sarah Franco [a,b], Amelia Stranz [a], Fiona Ljumani [a], Go Urabe [a], Mirnal Chaudhary [a,b], Danielle Stewart [a], Vijaya Satish Pilli [a], Matthew Kelly [a], Dai Yamanouchi [a], K. Craig Kent [a], Bo Liu [a,c,*]

[a] Department of Surgery, School of Medicine and Public Health, University of Wisconsin, Madison, WI 53705, USA
[b] Department of Cellular and Molecular Pathology, School of Medicine and Public Health, University of Wisconsin, Madison, WI 53705, USA
[c] Department of Cellular and Regenerative Biology, School of Medicine and Public Health, University of Wisconsin, Madison, WI 53705, USA

ARTICLE INFO

Keywords:
Biological sciences
Cell biology
Molecular biology
Pathophysiology
Pathology
FOXM1
Intimal hyperplasia
Smooth muscle cell
Proliferation
Apoptosis

ABSTRACT

Background: Accelerated smooth muscle cell (SMC) proliferation is the primary cause of intimal hyperplasia (IH) following vascular interventions. Forkhead Box M1 (FOXM1) is considered a proliferation-associated transcription factor. However, the presence and role of FOXM1 in IH following vascular injury have not been determined.

Objective: We examined the expression of FOXM1 in balloon-injured rat carotid arteries and investigated the effect of FOXM1 inhibition in SMCs and on the development of IH.

Methods and results: FOXM1 was detected by immunofluorescent staining in balloon-injured rat carotid arteries where we observed an upregulation at day 7, 14, and 28 compared to uninjured controls. Immunofluorescence staining revealed FOXM1 coincided with proliferating cell nuclear antigen (PCNA). FOXM1 was also detectable in human carotid plaque samples. Western blot showed an upregulation of FOXM1 protein in serum-stimulated SMCs. Inhibition of FOXM1 using siRNA or chemical inhibition led to the induction of apoptosis as measured by flow cytometry and western blot for cleaved caspase 3. Perturbations in survival signaling were measured by western blot following FOXM1 inhibition, which showed a decrease in phosphorylated AKT and β-catenin. The chemical inhibitor thiostrepton was delivered by intraperitoneal injection in rats that underwent balloon injury and led to reduced intimal thickening compared to DMSO controls.

Conclusions: FOXM1 is an important molecular mediator of IH that contributes to the proliferation and survival of SMCs following vascular injury.

1. Introduction

Cardiovascular diseases remain the leading cause of death worldwide [1]. Despite available surgical interventions such as balloon angioplasty and implantation of drug-eluting stents to treat occluded blood vessels, restenosis remains a primary impediment to the long-term efficacy of these interventions. Restenosis is the re-narrowing of vessels following revascularization interventions and results due to arterial damage and the subsequent cascade of aberrant signaling leading to intimal hyperplasia (IH) [2]. IH is a complex process involving smooth muscle cell (SMC) migration and proliferation and is the primary contributor to restenosis. In response to vascular injury, medial SMCs undergo a phenotypic switch from a quiescent, differentiated state to a synthetic, dedifferentiated status associated with a proliferative and migratory phenotype [3]. These changes result in a thickened, highly cellular neointima that ultimately leads to the re-narrowing of the vessel lumen [4, 5, 6].

FOXM1 is a member of the forkhead box protein family, which consists of a large family of transcription factors with a conserved winged helix/forkhead DNA binding domain and are crucial during development and in adult tissue homeostasis [7, 8]. Best studied in cancer biology, FOXM1 is considered a proliferation-associated transcription factor. It has been shown to promote cell cycle entry and proliferation via regulation of genes controlling G1/S transition, S-phase progression, G2/M transition, and proper mitotic execution [9]. Furthermore, FOXM1 has been shown to play a role in a variety of biological processes, including proliferation, migration, invasion, and inflammation, and has been shown to be aberrantly upregulated in the vast majority of cancers [10].

* Corresponding author.
E-mail address: liub@surgery.wisc.edu (B. Liu).

https://doi.org/10.1016/j.heliyon.2020.e04028
Received 7 August 2019; Received in revised form 15 March 2020; Accepted 15 May 2020

Loss of FOXM1 has been associated with numerous mitotic defects, including chromosome amplification, multipolar spindles, and misaligned chromosomes. These abnormalities often lead to senescence or mitotic catastrophe, which ultimately induces apoptosis [11, 12, 13].

Deregulation of the cell cycle is the basis of uncontrolled proliferation. As a corollary, recent studies have focused on the role of FOXM1 in SMC pathology in pulmonary hypertension, where vascular remodeling due to SMC proliferation is noted [14, 15]. Additionally, it was previously reported that inhibition of FOXM1 in cultured SMCs leads to G2/M arrest and decreased proliferation. Furthermore, smooth muscle-specific knockout of FOXM1 increased apoptosis in newborn mice [16].

Although these studies provide compelling evidence of the importance of FOXM1 in SMCs during development and disease, the role of this transcription factor in vascular injury induced by endovascular treatments such as balloon angioplasty has not been explored. In the present study, we used the rat carotid balloon injury model to identify the expression pattern of FOXM1 in the carotid wall. Furthermore, we targeted FOXM1 using specific inhibitors to elucidate the consequence of FOXM1 inhibition in vascular smooth muscle cells as well as in the balloon injury model. Our results demonstrated that FOXM1 expression is upregulated in injured vessels in a transient manner in both SMCs and endothelial cells. Our data also showed that inhibition of FOXM1 in SMCs results in apoptosis and is associated with perturbed survival signaling. Lastly, we found that FOXM1 inhibition *in vivo* by thiostrepton attenuated intimal thickening following balloon injury.

2. Materials and methods

2.1. Human carotid plaque tissue

Arterial tissues were obtained from 2 patients who had undergone open surgery at the University of Wisconsin Hospital for stenosis. Patients had no known connective tissue disorder, aortic dissection, or infection. Written informed consent was obtained from all patients prior to their participation. The study was performed under the protocol approved by the Institutional Review Committee at the University of Wisconsin-Madison (IRB No. 2011-0692) and conformed to the ethical guidelines of the Office of Research Compliance and Human Research Protection Program.

2.2. Rat carotid balloon injury

Male Sprague-Dawley rats 9–12 weeks old (~280–350g) underwent balloon injury of the left common carotid artery as described previously [17]. Briefly, following anesthetization, the left common, external, and internal carotid arteries were exposed and dissected. The external carotid was ligated and a small incision was made to insert a 2F catheter. The catheter was passed beyond the bifurcation into the common carotid artery, inflated to 2 ppm, retracted to the insertion point and then deflated. This process was repeated 3 times before ligating the external carotid and closing the incision. Rats were sacrificed at 3, 7, 14, and 28 days post-injury via perfusion fixation with 4% paraformaldehyde delivered by injection through the left ventricle using a syringe. Contralateral sides were used as uninjured controls. Unless stated otherwise, at least 3 animals were used for each group. All animal experiments were performed under protocols approved by the Institutional Animal Care and Use Committee (Protocol M005894) and Institutional Biosafety Committee (Protocol ID: B00000053) at the University of Wisconsin-Madison. All experiments were conducted according to the ethical guidelines of the Research Animal Resources and Compliance Guide for the Care and Use of Laboratory Animals.

2.3. Reagents

Thiostrepton was purchased from Millipore Sigma (598226) and was reconstituted in DMSO at a stock concentration of 1 mM and used at concentrations ranging from 0.5 μM to 1.5 μM. FDI-6 was purchased from Millipore Sigma (SML1392) and was reconstituted in DMSO at a stock concentration of 5 mM and was used at concentrations ranging from 2.5 μM to 10 μM. Z-VAD-FMK was purchased from Bachem (N-1510) and was reconstituted in DMSO.

2.4. Morphometric analysis and immunohistochemistry

After 3, 7, 14, or 28 days post-surgery rats were anesthetized and carotid arteries were fixed by perfusion with 4% paraformaldehyde via syringe injection. After immersion fixation overnight, the arteries were cut into 3 pieces and embedded into paraffin blocks so that each cut piece would be exposed to the microtome blade and analyzed together to account for variation in injury across the entire vessel area. The arteries were then sectioned into 5 μm sections and mounted onto 8 slides. Three slides (slide #1, #4, and #8) were stained with hematoxylin-eosin. The cross-sectional areas of the arterial wall, including the lumen area, intimal area, and medial area, were quantified by using NIH Image J program and the intima-to-media (I/M) ratios were calculated for immunofluorescent staining, slides were permeabilized with 0.1% Triton X-100 and underwent heat-induced antigen retrieval (Citrate buffer pH 6.0 or Tris-EDTA pH 9). Staining was performed using anti-FOXM1 from Santa Cruz (sc-500; 1:100) for the main figures and AVIVA (ARP39518_P050; 1:75) for supplemental figures, anti-PCNA from Santa Cruz (sc-56; 1:100), anti-CD31 from R&D Systems (AF3628; 1:250), or no primary controls and slides were incubated overnight at 4 °C. Slides were then washed 3x with PBS and incubated in Alexa Fluor (Thermo Scientific) secondary antibodies at a concentration of 1:200 for 1h at room temperature. Injured sections were imaged using the same settings as their respective uninjured controls; images of each time point were taken separately. Any adjustments to brightness were kept consistent between control and injured sets.

2.5. Thiostrepton intraperitoneal injection

Thiostrepton was dissolved in DMSO at a concentration of 25 mg/ml (15.0159 mM), aliquoted, and stored at -20 °C. Aliquots were thawed only once on the day of injection. Rats were weighed daily and thiostrepton or DMSO was diluted in PBS to adjust for a 15 mg/kg injection. On the day of surgery, rats were injected at the start of surgery (approximately 1 h prior reestablishing blood flow in the injured carotid arteries). Rats were then weighed and injected with 15 mg/kg thiostrepton or equivalent DMSO once daily for the duration of the experiment.

2.6. Cell culture

Rat A-10 cells were purchased from ATCC (ATCC CRL-1476) and used at passages 20–30. Cells were maintained at 37 °C with 5% CO2 in Dulbecco's Modified Eagle's Medium (DMEM) modified to contain 4 mM L-glutamine, 4500 mg/L glucose, 1 mM sodium pyruvate, and 1500 mg/L sodium bicarbonate (ATCC 30–2002) supplemented with 10% FBS from Gibco BRL Life Technologies (Carlsbad, CA), 100 U/mL penicillin, and 100 U/mL streptomycin. For experiments, primary rat aortic SMCs were isolated according to a previously described method [18]. Primary cells were maintained at 37 °C with 5% CO2 in DMEM purchased from Thermo Scientific (11054020) supplemented with 10% FBS, 100 U/mL penicillin, and 100 U/mL streptomycin. Primary cells were used at passages 3–6.

2.7. siRNA transfection

A-10 cells were seeded at 52,000 cells per well in a 6 well plate and allowed to attach for 16–24h. siRNA was complexed with Lipofectamine RNAi max (Thermo Fisher Scientific, Rockford, IL) 10 min prior to adding to cells. For complexation with RNAi max: in one vial, 10nM siRNA or

scramble control was diluted in Optimem (100 μL), and in another vial, 4 μL of RNAi max was diluted in Optimem (100 μL). The Lipofectamine RNAi max solution was added to the siRNA solution and mixed by pipetting. The siRNA/liposome complexes were incubated at room temperature for 10 min then added to the 2mL of complete growth medium in the wells. Cells were incubated with the mixture for 4 h then replaced with fresh medium. As a control, one well of cells included transfection reagent only without siRNA (indicated as sham). Cells were incubated for 48 h before collection for analysis. Rat FOXM1 siRNA duplexes were purchased from Origene (SR503608). The following specific siRNA sequences used were and compared against a scramble control (product No. SR30004):

SiFOXM1(1): GCUAGCACAAGAACACUACUGUAAC (exon 6/7)
SiFOXM1(2): ACAUUGGACCAAGUGUUUAAGCCAC (exon 8)
SiFOXM1(3): ACAGCAGAAACGACCCAAUCCUGAG (exon 9)

2.8. Quantitative real-time PCR (qRT-PCR)

Total RNA was extracted from cultured cells using TRIzol Reagent (Thermo Fisher Scientific, Waltham, MA). 750 ng-1 μg of RNA was used for the first-strand cDNA synthesis (Applied Biosystems, Carlsbad, CA). A no-RT (reverse transcriptase) control was included in the same PCR mixtures without reverse transcriptase to confirm the absence of DNA contamination in RNA samples. qPCR primers for FOXM1 and GAPDH were as follows:

Rat FOXM1: Fwd-GGACCATTCACCCAAGTGCT; Rev-CGCCTAG TGGGAGTTCAGTT

Rat GAPDH: Fwd-AGACAGCCGCATCTTCTTGT; Rev-CTTGCCG TGGGTAGAGTCAT

Duplicate of 20 μl reactions were carried out in 96-well optical reaction plates using SYBR® Green PCR Master Mix (Applied Biosystems, Carlsbad, CA) with gene-specific primers and the qPCR was run in the 7500 Fast Real-Time PCR System (Applied Biosystems, Carlsbad, CA). Amplification of each sample was analyzed by melting curve analysis, relative differences in each PCR sample were corrected using GAPDH mRNA as an endogenous control and normalized to the level of control by using the 2-ΔΔCt method.

2.9. Immunoblotting

When samples were collected for detection of cell death, cells were harvested by trypsinization and centrifugation (including floating cells). For all other protein detection, samples were harvested by direct lysis in the dish. Cells were lysed with RIPA buffer (Sigma-Aldrich, St. Louis, MO) containing Halt Cocktail with phosphatase and protease inhibitors (Thermo Scientific, Rockford, IL). Protein concentration was determined by Bio- Rad DC Protein Assay kit (Hercules, CA). Equal amounts of protein (15-20ug) were loaded onto SDS-PAGE gels. After separation, samples were transferred to polyvinylidene fluoride (PVDF) membranes (Bio-Rad, Hercules, CA). Membranes were blocked in 5% skim milk with TBS-T for 1 h at room temperature followed by incubation in primary antibodies overnight at 4 °C. Protein levels were assessed using the following primary antibodies: FOXM1 1:1000 (Santa Cruz sc-500 and sc-271746), cyclin A 1:250 (Santa Cruz sc-596), survivin (Santa Cruz sc-17779), phospho-AKT ser 473 1:2000 (CST 4060), total AKT 1:2000 (CST 4691), β-catenin 1:250 (Santa Cruz sc-7963), non-phospho active β-catenin 1:1000 (CST 8814S), beta-actin 1:8000, and GAPDH 1:8000. Of note, sc-500 and sc-271746 recognize all isoforms of FOXM1, which often appears as multiple bands at approximately 100–110kDa. Membranes were washed 3x in TBS then incubated for 1 h at room temperature with horseradish peroxidase-conjugated secondary antibodies. Membranes were visualized using the Clarity Western ECL Substrate system (Bio-Rad, Hercules, CA) or SuperSignal™ West Femto Maximum Sensitivity Substrate (Thermo Scientific, Rockford, IL) and imaged using a FujiFilm Image-Quant LAS-4000 imager. Image Studio Lite Ver 5.2 was used to quantify western blots. For FOXM1, when multiple bands appeared, the density was measure cumulatively for all bands.

2.10. Thymidine synchronization

In order to synchronize A-10 cells, we utilized a previously published protocol detailing this methodology in A-10 cells [19; Harper, J.V. Chapter 10]. Briefly, to block cells at the G1/S border, A-10 cells were cultured in complete medium containing 2 mM thymidine for 12h (first thymidine block). Cells were washed 3x with PBS, and medium was replaced with complete medium for 12h. Medium was then replaced with medium containing 2 mM thymidine for an additional 12h (second thymidine block). Following the second thymidine block, cells were washed 3 times with PBS and released into complete growth medium for indicated time points and cells were collected for protein.

2.11. Cell titer glo assay

The CellTiter-Glo® Luminescent Cell Viability Assay was obtained from Promega. Cells were seeded 2,000 cells per well on a 96-well plate and allowed to attach for 16–24h. The next day cells were treated with concentrations of FDI-6 ranging from 2-10 μM for 24h. Cell titer glo reagents were added according the manufacture's protocol. Absorbance was measured using the Flexstation 3 (Molecular Devices, LLC., San Jose, CA). At least 4 well per condition were measured.

2.12. Flow cytometry analysis

Cell death was evaluated by flow cytometry using an Annexin V-PE/7-AAD staining Kit (BD Biosciences, San Jose, CA). Medium containing floating cells was moved to 15 ml conical tubes. Cell culture dishes were washed with PBS and trypsinized at 37 °C. The detached cells were combined with the floating cells and collected by centrifugation (1500 rpm for 5 min). Cell pellets were further washed twice with ice-cold PBS and resuspended in 100 μl binding buffer from the Annexin V-PE/7-AAD staining kit. 5 μl of PE Annexin-V and 5 μl of 7-AAD were added to the cells and incubated at room temperature for 15 min. After incubation, 400 μl binding buffer was added to each sample. Cells were analyzed using a Becton Dickinson Biosciences FACSCalibur (BD Biosciences, San Jose, CA).

2.13. Statistical analysis

Data are presented as mean ± SEM when n = 3 or more. Datasets containing n = 2 show standard deviation of technical or biological replicates. One-way ANOVA with Fisher's Least Significant Difference post-hoc test was used to compare 3 or more means. Comparisons between vehicle and drug applications *in vivo* were made using a non-paired Student's t-test. Statistical analyses were performed using GraphPad Prism 8. Differences with $P < 0.05$ were considered statistically significant.

3. Results

3.1. Vascular injury triggers arterial expression of FOXM1

To investigate the role of FOXM1 in the development of IH following vascular injury, we subjected adult rats to carotid balloon injury. The formation of neointima was observed by day 7 and increased through day 14 and 28 post-injury (Supplemental Figure S1). Immunohistochemical analysis showed comparable FOXM1 accumulation in injured and control arteries at day 3 post-injury (Figure 1A). However, there was a clear elevation of FOXM1 at day 7 within the neointima of injured arteries (Figure 1B). Augmented FOXM1 was still detectable at day 14 and 28 (Figure 1C, D, respectively); however, cells expressing FOXM1 were

primarily localized in the intima layer most proximal to the lumen at these time points.

To further establish the clinical relevance of FOXM1 in arterial injury, we obtained two carotid plaque samples from patients who had undergone open surgery for stenosis. Immunohistochemical analysis revealed FOXM1 expression was present in the vascular wall and was primarily localized to the cytoplasm of cells (Figure 1E). The specificity of FOXM1 staining in balloon-injured and patient-derived arteries was confirmed using an alternative FOXM1 antibody (Supplemental Figure S2). Taken together, these findings suggest a role for FOXM1 in the development of IH as well as in human atherosclerotic plaques where SMCs have previously been shown to undergo pathological transition.

3.2. FOXM1 is expressed in smooth muscle cells and endothelial cells in balloon-injured arteries

We sought to identify which cell types express FOXM1 in the injured vessel wall. Given that neointima formation is primarily an SMC pathology and our findings that FOXM1 was highly expressed in the neointima at day 7, we co-stained day 7 sections with FOXM1 and α-SMA, a vascular SMC marker. Results showed that most of the FOXM1 positive cells were also positive for α-SMA (Figure 2A).

To determine whether FOXM1 is also expressed in endothelial cells, we assessed the presence of FOXM1 at day 14 and day 28 post-injury, times at which the injured artery may be re-endothelialized. CD31-positive cells in injured arteries displayed FOXM1 expression both at day 14 and day 28 (Figure 2B, C, respectively). FOXM1 was not detected in the intact endothelium from uninjured controls (data not shown). Taken together, our results show that FOXM1 is upregulated primarily in neointimal SMCs but also present in the re-endothelialized layer of the vessel following injury.

3.3. FOXM1 expression is elevated in proliferating smooth muscle cells in vivo and in vitro

FOXM1 is characterized as a proliferation-associated transcription factor [9, 20]. Thus, we asked if FOXM1 expression corresponds with cell proliferation during the development of IH. Immunohistochemistry was performed to examine the expression of FOXM1 and proliferating cell nuclear antigen (PCNA), a marker of proliferation, 7 days after injury when cell proliferation is prominent. Our results revealed that FOXM1 and PCNA are co-expressed in the SMC-rich neointimal layer of injured rat carotid arteries (Figure 3A).

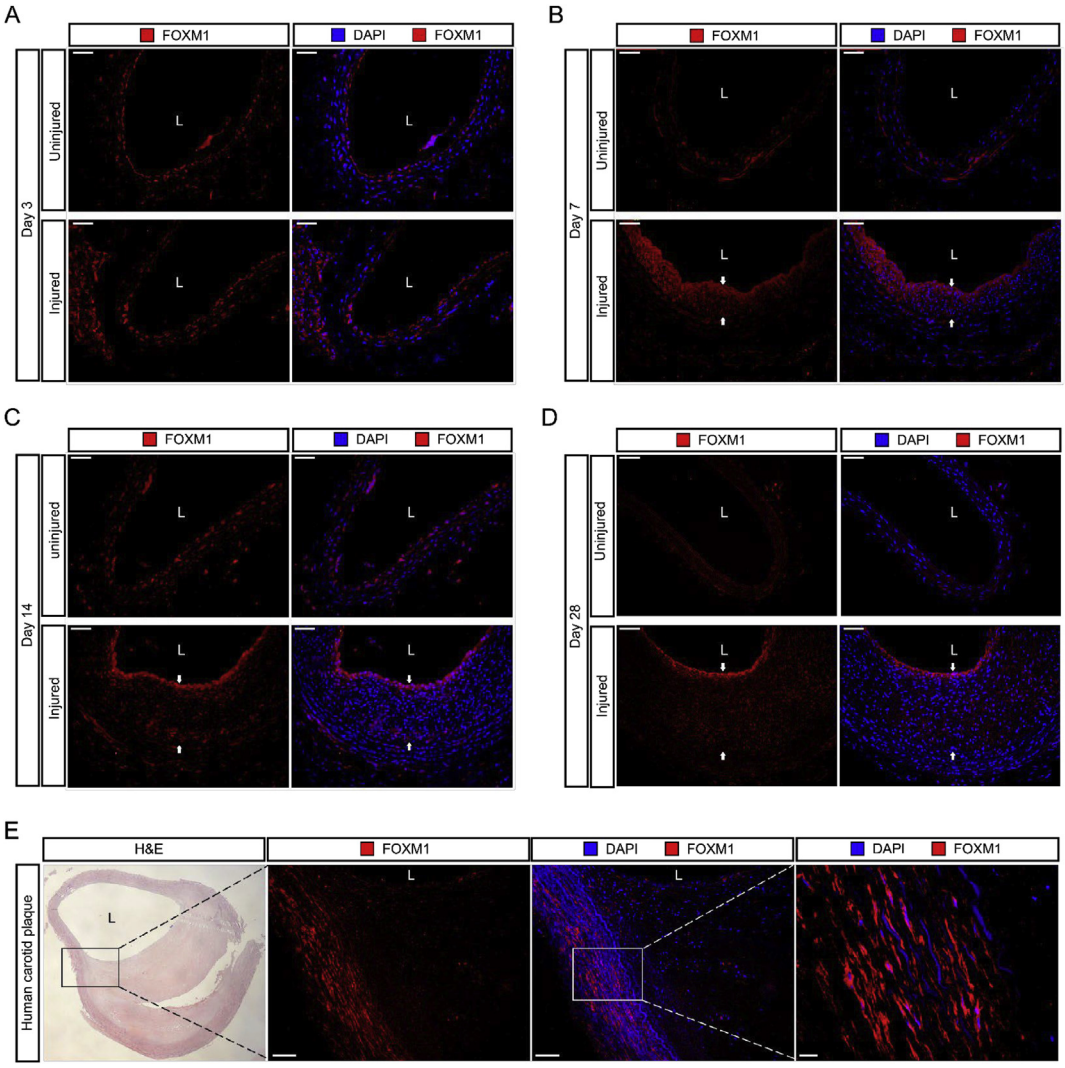

Figure 1. Vascular injury triggers FOXM1 arterial expression. Expression of FOXM1 in carotid arteries from uninjured or balloon-injured rats. Representative photographs of immunohistochemistry analysis for FOXM1 (red) and DAPI (blue) are shown for (A) day 3, (B) day 7, (C) day 14, (D) and day 28. Scale bars 50 μm. (E) Immunohistochemistry for FOXM1 (red), and DAPI was performed on human carotid plaque sections. Scale bars 100 μm and 20 μm. L indicates lumen. White arrows demarcate neointima. Santa Cruz sc-500 anti-FOXM1 antibody was used for staining.

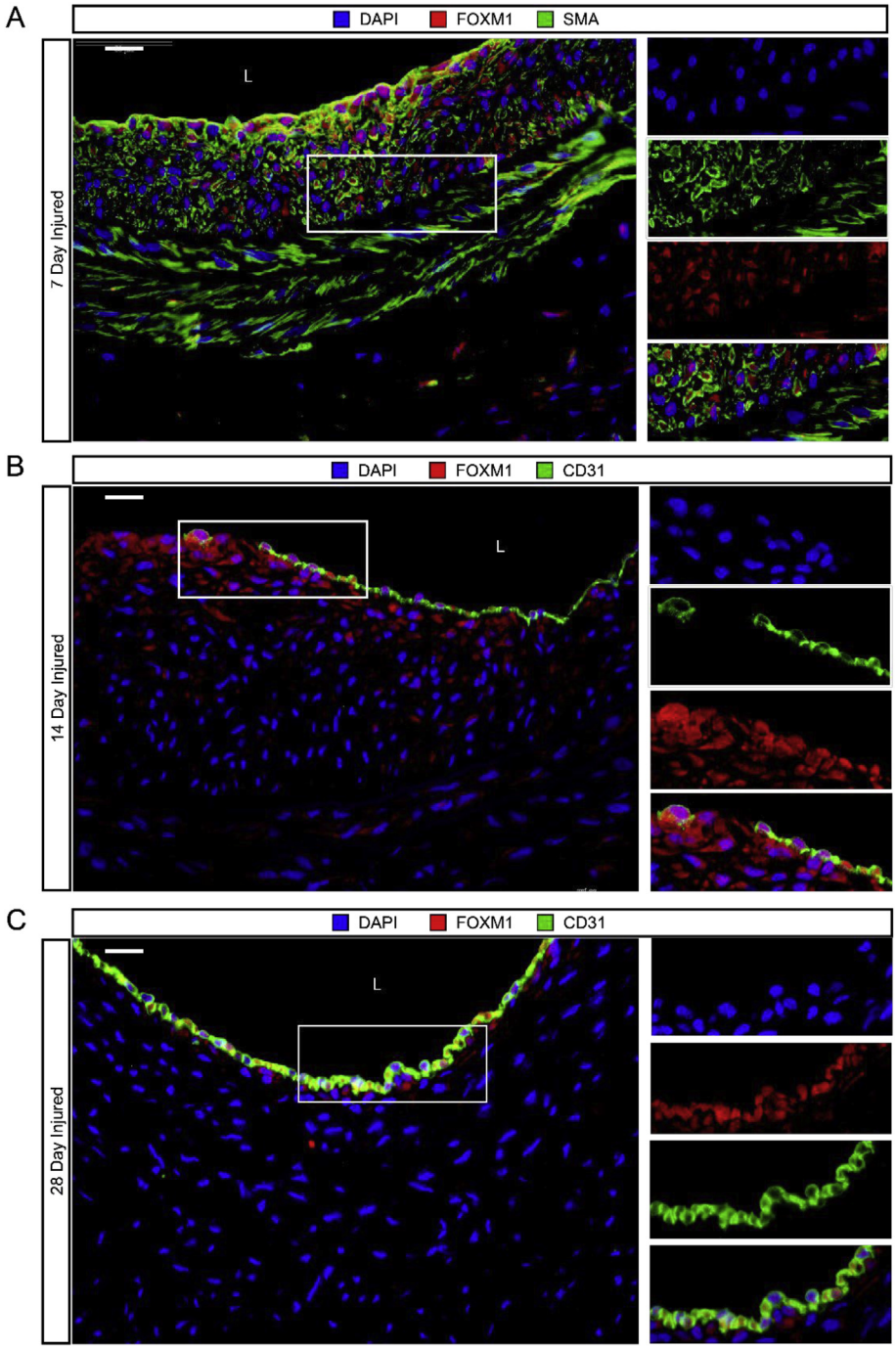

Figure 2. FOXM1 is expressed in smooth muscle cells and endothelial cells in balloon-injured arteries. Representative immunofluorescent staining of balloon injured carotid arteries. (A) Confocal images of FOXM1 (red), alpha-smooth muscle actin (SMA) (green), and DAPI (blue) co-stain on day 7 injured sections. (B) Immunofluorescent images of FOXM1 (red), CD31 (green), and DAPI (blue) co-stain on day 14 injured sections. (C) Immunofluorescent images of FOXM1 (red), CD31 (green), and DAPI (blue) co-stain on 28 day injured sections. Scale bars 25 μm. L indicates lumen.

The high rates of SMC proliferation are transient and generally return to near basal levels by day 14 and beyond due, in part, to re-endothelialization. This was confirmed by immunohistochemistry on day 14 (Figure 3B) and day 28 (Figure 3C) samples, which showed lower expression levels of PCNA compared to day 7 and revealed that FOXM1 expression was primarily limited to PCNA positive cells at these time points and had a similar transient expression as PCNA.

To further examine the role of FOXM1 in SMCs, we analyzed the expression levels of FOXM1 *in vitro* using various sources of SMCs. To mimic the *in vivo* state of SMCs, we made cells quiescent by serum deprivation for 48h then stimulated cells with serum to re-enter the cell cycle and proliferate. We found that compared to quiescent cells, serum-stimulated A-10 (Supplemental Figure S3A), A7R5, primary rat aortic, and primary rat carotid cells expressed higher levels of FOXM1 (Figure 3D). We chose to conduct all following experiments in A-10 cells since they are characteristically similar to neointimal SMCs. We explored the cell cycle-dependent expression of FOXM1 by synchronizing SMCs at the G1/S boundary by double thymidine block followed by release into the cell cycle. Similar to other reports [21, 22], FOXM1 protein levels rose in a time-dependent manner following thymidine release and appeared to peak between 5- 7 h post-release (Figure 3E; Supplemental Figure S3B). This increase was accompanied by a similar transient expression pattern of cyclin A, which was previously shown to rise throughout the S phase in A-10 cells [19]. Survivin, which peaks at the G2/M phase [19], showed highest expression at 7–12 h post-release (Supplemental Figure S3B). Collectively, these data show that FOXM1 expression corresponds with the proliferative status of vascular SMCs.

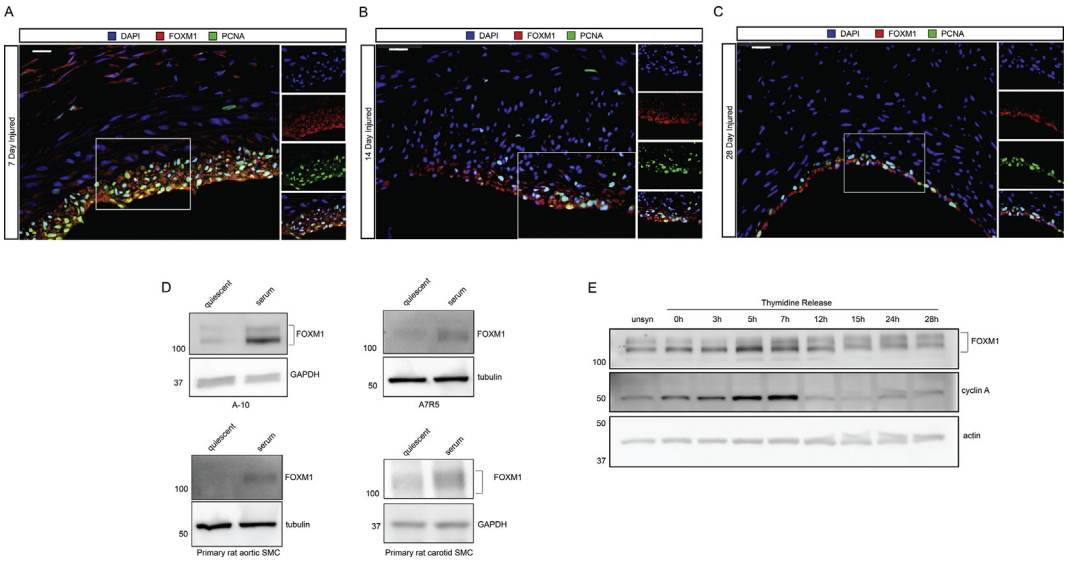

Figure 3. FOXM1 is elevated in proliferating smooth muscle cells in vivo and in vitro. Immunohistochemistry analysis for FOXM1 (red), PCNA (green), and DAPI (blue) was performed on injured carotid arteries. (A) Representative images for confocal microscopy on day 7 sections are shown. Representative images for fluorescent microscopy on (B) day 14 and (C) day 28 are shown. Scale bars 50 μm. The right panels are zoomed-in views of the areas outlined by white rectangles. (D) SMCs were made quiescent by serum deprivation for 48h then stimulated with 10% FBS for 18h. Representative western blots for FOXM1 are shown (n = 3 A-10 cells; n = 1 A7R5 cells; n = 2 primary rat aortic cells; n = 1 primary rat carotid cells). (E) A-10 cells were synchronized by double thymidine block then released into serum and collected at indicated time points. Representative western blot for FOXM1, cyclin A, and actin are shown (n = 2). Full non-adjusted images for western blots are shown in Supplementary Material.

3.4. FOXM1 inhibition in vascular SMCs triggers apoptosis

To investigate the effects of FOXM1 inhibition in SMCs, we knocked down FOXM1 by RNA interference (RNAi). Efficient knockdown was confirmed by western blot (Figure 4A) and qRT-PCR (Figure 4B). Flow cytometry analysis for Annexin V and 7-AAD showed a significant increase in the apoptotic population in siRNA-treated cells compared to untreated or scramble controls (Figure 4C). Western blot analysis revealed high levels of cleaved caspase 3 in siRNA-treated cells compared to the scramble group (Figure 4D; Supplemental Figure S4A).

Thiostrepton is a well-characterized FOXM1 inhibitor that has been shown to inhibit both FOXM1 expression and activity [23, 24, 25]. Treatment with thiostrepton prior to serum stimulation led to a dose-dependent reduction in FOXM1 protein levels (Figure 4E; Supplemental Figure S4C). We also observed a significant increase in apoptosis in thiostrepton-treated cells compared to untreated or DMSO-treated cells (Figure 4F). In addition, pre-treatment with 80uM z-VAD-fmk, a pan-caspase inhibitor, abrogated cell death induced by thiostrepton treatment (data not shown). Cleaved caspase 3 was abundantly expressed following treatment with thiostrepton (Figure 4G; Supplemental Figure S4C).

Next, we examined the effect of the small molecule inhibitor FDI-6. Similar to thiostrepton, FDI-6 has been shown to be a selective antagonist of FOXM1 [26]. Cell Titer Glo viability assay showed a dose-dependent decrease in cell survival in cells treated with FDI-6 (Figure 4H). Cleaved caspase 3 was also detected following treatment with FDI-6 (Figure 4I; Supplemental Figure S4D). In summary, these data provide strong evidence that inhibition of FOXM1 in SMCs leads to apoptosis.

3.5. Inhibition of FOXM1 perturbs survival signaling

To ascertain if the cell death response observed after FOXM1 inhibition was accompanied by corresponding changes in survival signaling pathways, we assessed protein levels of two survival proteins. PI3K/AKT and β-catenin signaling pathways are important regulators of SMC survival and proliferation following vascular injury [27, 28, 29, 30]. As shown in Figure 5A, PDGF activated AKT pathway as evidenced by AKT phosphorylation. Inhibition of FOXM1 via siRNA significantly ablated AKT activation in PDGF-stimulated SMCs. Accordingly, pre-treatment with thiostrepton reduced levels of PDGF-stimulated phospho-AKT compared to the DMSO control (Figure 5B).

Concomitantly, we found that inhibition of FOXM1 via RNAi also decreased total levels of β-catenin (Figure 5C). A similar reduction in active β-catenin levels was also observed in cells treated with thiostrepton (Figure 5D) and FDI-6 (Figure 5E). Collectively, these data show that FOXM1 is critical for SMC survival.

3.6. Thiostrepton mitigates intimal thickening following balloon injury

Next, we assessed the effect of FOXM1 inhibition on the formation of intimal hyperplasia following balloon injury. Rats were administered 15 mg/kg thiostrepton daily for 14 days following balloon injury. Measurements of body weight showed a decrease in the weight of animals receiving thiostrepton (data not shown). However, animals appeared healthy otherwise. Carotid arteries were harvested at 2 weeks and subjected to immunohistochemical analysis. We observed neointima formation in both DMSO and thiostrepton-treated rats (Figure 6A).

Morphometric analysis of H&E sections revealed that thiostrepton, without significantly reducing the media (Figure 6B), significantly reduced the intima area compared to DMSO controls (Figure 6C). The lumen area showed a slight increase in thiostrepton-treated rats, although results were not statistically significant (Figure 6D). The intima to media ratio was not statistically different between thiostrepton and DMSO groups (Figure 6E). Taken together, our results indicate that thiostrepton has a moderate inhibitory effect on neointima formation.

4. Discussion

In this study, we presented evidence of elevated FOXM1 in balloon-injured carotid arteries and in the vessel wall of human carotid plaque samples from patients who had undergone open surgery for stenosis.

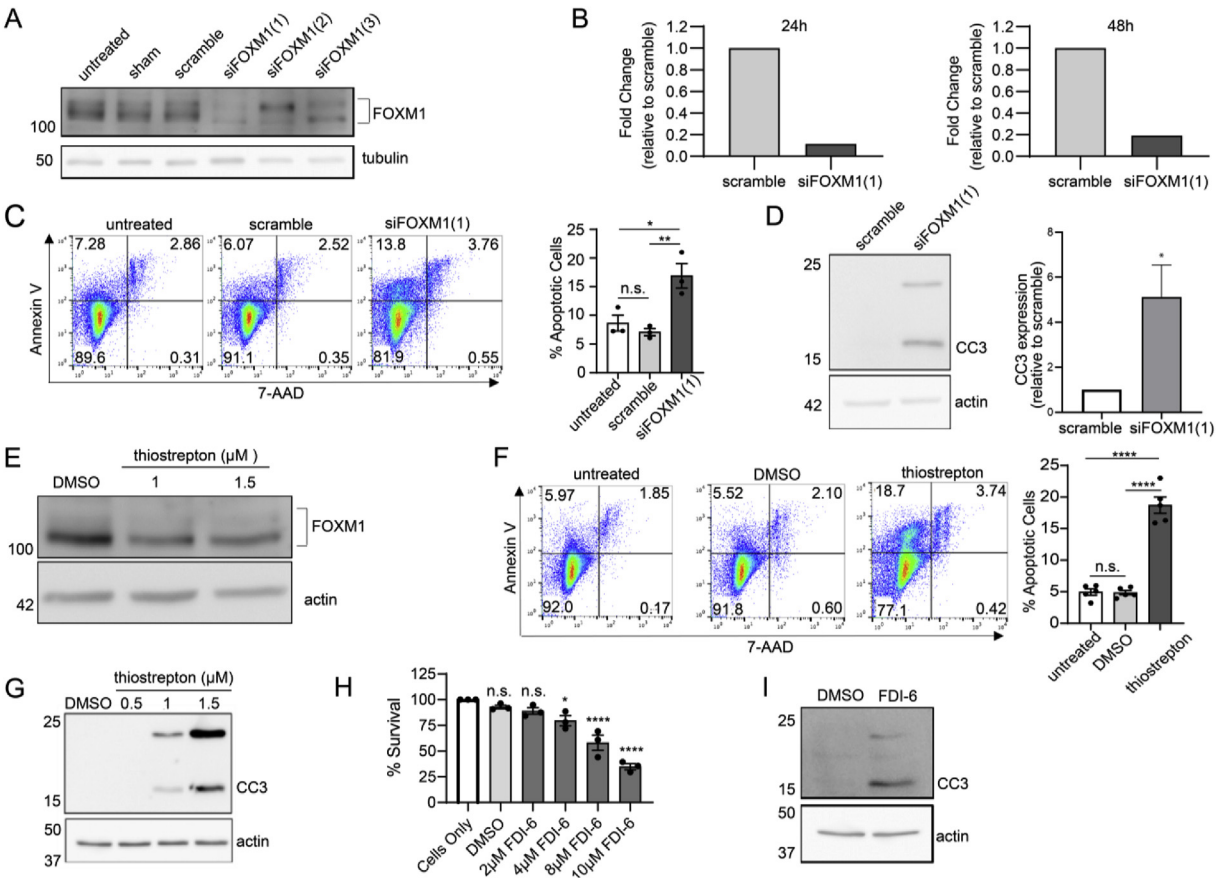

Figure 4. FOXM1 inhibition in vascular smooth muscle cells induces apoptosis. (A) Representative western blot (WB) analysis of FOXM1 protein levels after siRNA knockdown of FOXM1 for 48h. Three different siRNAs (1, 2, 3) targeting FOXM1 were used (n = 2 for siFOXM1(2); n = 3 siFOXM1(1) and (3)). All further experiments utilize siFOXM1(1). (B) qRT-PCR analysis for FOXM1 mRNA following siRNA knockdown of FOXM1 for 24h (left) or 48h (right) (n = 2). Data were normalized to GAPDH expression and are expressed as fold change of scramble control. (C) Flow cytometry analysis for Annexin V/7-AAD on cells that were untreated, transfected with scramble, or siFOXM1. Quantification is percent apoptotic cells (Annexin V positive) (n = 3) *P = 0.0194, **P = 0.0088. (D) Representative WB analysis and quantification for cleaved caspase 3 (CC3) levels after siRNA knockdown of FOXM1 for 48h. Expression normalized to the housekeeping protein and the scramble control was set to 1 (n = 3)+SEM *P = 0.0276. (E) Representative WB for FOXM1 levels. Cells were serum deprived for 24h, pre-treated with 1 μM thiostrepton for 1h, then serum was added for 18h (n = 3) (F) Flow cytometry analysis for Annexin V/7-AAD on cells that were untreated, treated with DMSO, or treated with 1 μM thiostrepton for 24h. Quantification is average percent apoptotic cells (n = 5) ****P < .0001. (G) Representative WB analysis for CC3 levels following 24h treatment with varying concentrations of thiostrepton (n = 3 for 1 μM and 1.5 μM). (H) Cell viability was measured by cell titer glo following treatment with FDI-6 at varying concentrations. Bar graph shows percent survival. Bars are SEM (n = 3). Treatment groups compared to cells only; *P = 0.0157, ****P < .0001. (I) Representative WB for CC3 levels following 24h treatment with 8 μM FDI-6 (n = 2). Full non-adjusted images for WBs are shown in Supplementary Material.

FOXM1 expression coincided with both α-smooth muscle cell actin (a smooth muscle cell marker) and CD31 (an endothelial cell marker) with the neointimal smooth muscle cells being the primary source of FOXM1 expression. In further histological examination, we found FOXM1 corresponded with the transient proliferation of neointimal smooth muscle cells following balloon injury. Western blotting corroborated this transient expression in cultured aortic smooth muscle cells that were either stimulated with serum or synchronized by double thymidine block. These studies suggested that FOXM1 might play a role in the proliferation of SMCs and, ultimately, the development of intimal hyperplasia following vascular injury. This notion is further supported by evidence of RNAi-mediated and chemical inhibition studies. Inhibition of FOXM1 led to SMC apoptosis and also antagonized PI3K/AKT and β-catenin survival pathways. More importantly, treatment with thiostrepton in the balloon injury model reduced intimal thickening. Taken together, these data suggest that FOXM1 may contribute to the injury-induced proliferation of SMCs and that targeting FOXM1 may ameliorate intimal hyperplasia.

FOXM1 is widely studied in developmental and cancer biology. It is characterized as a proliferation-associated transcription factor because its expression is limited to proliferating cells and extinguished in the majority of adult and differentiated cells [31]. Numerous studies in the cancer field have implicated FOXM1 in regulating cellular proliferation, cell cycle activation, migration, and apoptosis resistance [10, 32, 33, 34, 35, 36, 37]. Many of these FOXM1-regulated biological processes that become abnormally activated in cancer cells are analogous to those in IH. For example, in a normal vessel wall, vascular SMC proliferation is scarcely detected; however, cell cycle activation and increased proliferation is observed in early atherogenesis, injured vessels, and in animal models of IH [38, 39]. Moreover, it has also been shown that FOXM1 plays an important role in SMC pathology in the context of pulmonary hypertension by contributing to the hyperproliferative and apoptotic-resistant phenotype of pulmonary artery SMCs [40]. Despite this, FOXM1 has not been interrogated in surgery-induced IH or restenosis. In this study, we demonstrated that FOXM1 is highly expressed in injured arteries when SMC proliferation is abundant, but not at day 3 when apoptosis has been shown to be present. This raises the possibility that FOXM1 is upregulated to counteract early apoptosis and may be acting as a proliferation and survival factor. Furthermore, our results showed that while FOXM1 is detectable at basal levels in cultured SMCs that have been made quiescent (a condition used to mimic SMCs in a healthy vessel), stimulating cells to re-enter the cell cycle and proliferate

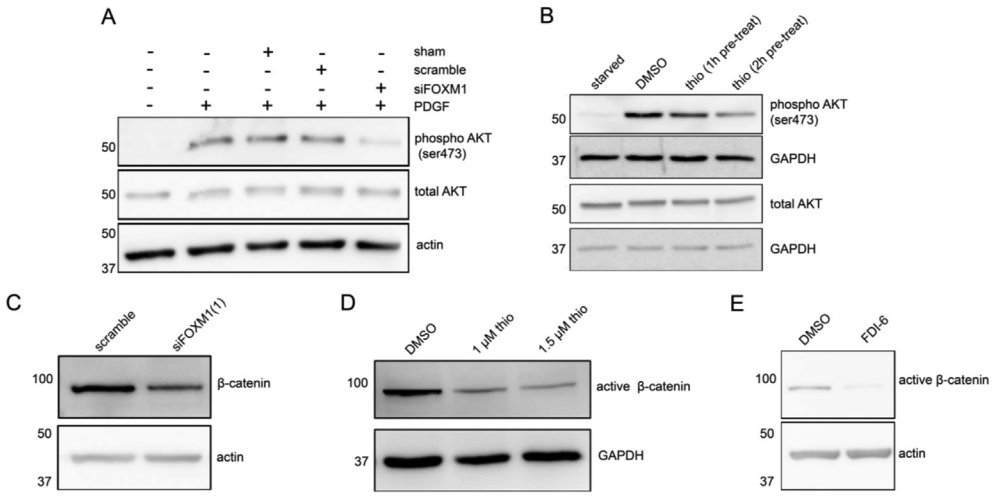

Figure 5. Inhibition of FOXM1 perturbs survival signaling. (A) Representative western blot for phospho AKT (ser473) and total AKT from cell lysates of untreated, sham (transfection reagent), scramble siRNA, or siFOXM1-treated cells. Cells were transfected for 24h, followed by 24h starvation, then stimulated for 20m with 10 ng/ml PDGF (n = 2). (B) Representative western blots for phospho AKT and total AKT from cell lysates of cells that were serum starved for 24h, pre-treated with 1 μM thiostrepton for 1 or 2h then stimulated with 20 ng/ml PDGF for 20m (n = 2). (C) Representative western blot for β-catenin from cell lysates of cells that were treated with scramble or siFOXM(1) for 48h (n = 2). (D) Representative western blot for active β-catenin from cell lysates of cells that were treated with 1 μM or 1.5 μM thiostrepton fror 24h (n = 2). (E) Representative western blot for active β-catenin from cell lysates of cells that were treated with 8 μM FDI-6 for 24h (n = 2). Full non-adjusted images for western blots are shown in Supplementary Material.

greatly increases FOXM1 expression. These data suggest a role for FOXM1 in vascular smooth muscle cell pathology.

The data reported here are centered around the role of FOXM1 in vascular SMCs and how it might drive IH formation through regulation of SMC proliferation. However, the overall process of restenosis is complex. Impaired endothelial repair, platelet adhesion, infiltration of inflammatory cells, and overall vessel remodeling can all promote vessel narrowing. Regarding endothelial cells, it has been shown that preserving endothelial integrity and function aids in preventing restenosis after angioplasty [41]. Intriguingly, we found that FOXM1 expression was expressed to a lesser extent in areas where re-endothelialization had occurred and high in denuded areas. We speculate this expression pattern is due to direct stimulation via factors in the blood. When endothelial cells have repaired, they form a barrier between the circulating blood and underlying SMCs, thus decreasing SMC exposure to mitogenic stimuli and FOXM1 expression. An alternative mechanism that may account for our observation is that endothelial cells, once repaired, suppress FOXM1 expression in SMCs. This paracrine crosstalk would be an interesting mechanism to explore considering the recent publication by Dai et al. [15] where they show that ECs produce factors which stimulate SMC expression of FOXM1. Future studies are warranted to explore this possibility. Interestingly, we found that FOXM1 expression persisted at day 28 but was primarily localized to the regenerated endothelium, and to some extent, in the area directly adjacent to the endothelial cells. This raises the question of whether FOXM1 might be a candidate gene for overexpression studies in endothelial cells to promote endothelial repair. Furthermore, studies have shown that modulating FOXM1 expression can diminish the ability of endothelial cells to repair [42]. In addition, FOXM1 also drives fibrogenesis through fibroblast proliferation [43] and is also required for macrophage migration in pulmonary inflammation, and macrophage recruitment in liver repair [43, 44]. These studies highly suggest that FOXM1 is likely to promulgate multiple processes involved in restenosis through mechanisms in other cell types besides SMCs. In future studies, emphasis should be put on understanding the role of FOXM1 in all vascular cell types as well as contributing circulating cells.

Forkhead factors have been shown to interact, modulate, or be regulated by many signaling pathways involved in development and disease. Some key signaling pathways that involve forkhead factors include hedgehog, MAP kinase, TGFβ/Smad3, PI3K/AKT, Wnt/β-catenin, and insulin/IGF [45, 46, 47]. These pathways have all been shown to contribute to SMC proliferation [48]. Regarding FOXM1, it has been demonstrated that PI3K inhibition leads to reduced FOXM1b transcriptional activity and FOXM1 expression [49, 50]. Moreover, tumor cells expressing activated AKT1 were shown to be addicted to FOXM1 [51]. FOXM1 has also been shown to activate PDGF-A and form a positive feedback loop in the PDGF/AKT signaling pathway [52]. In line with this evidence supporting FOXM1 crosstalk with PI3K/AKT signaling, our results demonstrate that FOXM1 inhibition causes AKT signaling dysfunction in SMCs. With respect to Wnt/β-catenin and FOXM1, it has been shown that FOXM1 promotes β-catenin nuclear localization as well as transcriptionally regulates β-catenin [53, 54]. Additionally, WNT signaling stabilizes FOXM1 [55]. Our data suggest FOXM1 may also interact with β-catenin in SMCs, evidenced by our results that FOXM1 inhibition reduces levels of both total β-catenin and active β-catenin. Future studies are needed to elucidate if FOXM1 directly interacts with β-catenin or exactly how FOXM1 modulates PI3K/AKT.

Recent evidence suggests thiostrepton treatment reduced vascular remodeling and decreased SMC proliferation in hypertensive rats [15]. Additionally, targeting FOXM1 by thiostrepton has been shown to inhibit tumor growth via the reduced proliferation of Ewing's sarcoma cells [56], as well as reduce breast and liver cancer xenografts likely through increased cell death [57]. Notably, our in vivo results demonstrated a moderate decrease in intimal thickening in rats treated with thiostrepton compared to DMSO controls. However, the effectiveness of thiostrepton varied between individual rats. We suspect that poor solubility of thiostrepton may account for the variability in the efficacy of decreased intima formation, as this may lead to discrepancies in bioavailability.

Although we also observed drastic weight loss in thiostrepton-treated rats, the variability in weights could not be correlated with the degree of reduction in intimal thickening. This prompts us to consider both toxicity and delivery routes of thiostrepton for future studies. Others have encapsulated thiostrepton in micelles to overcome solubility issues [57]. Alternative delivery methods such as pluronic gel or intraluminal delivery at the site of injury should also be considered. Lastly, considering that thiostrepton is a proteasome inhibitor, it is likely to affect other proteins and potentially the growth and function of various organs. Thiostrepton interacts with FOXM1 to prevent its binding to its

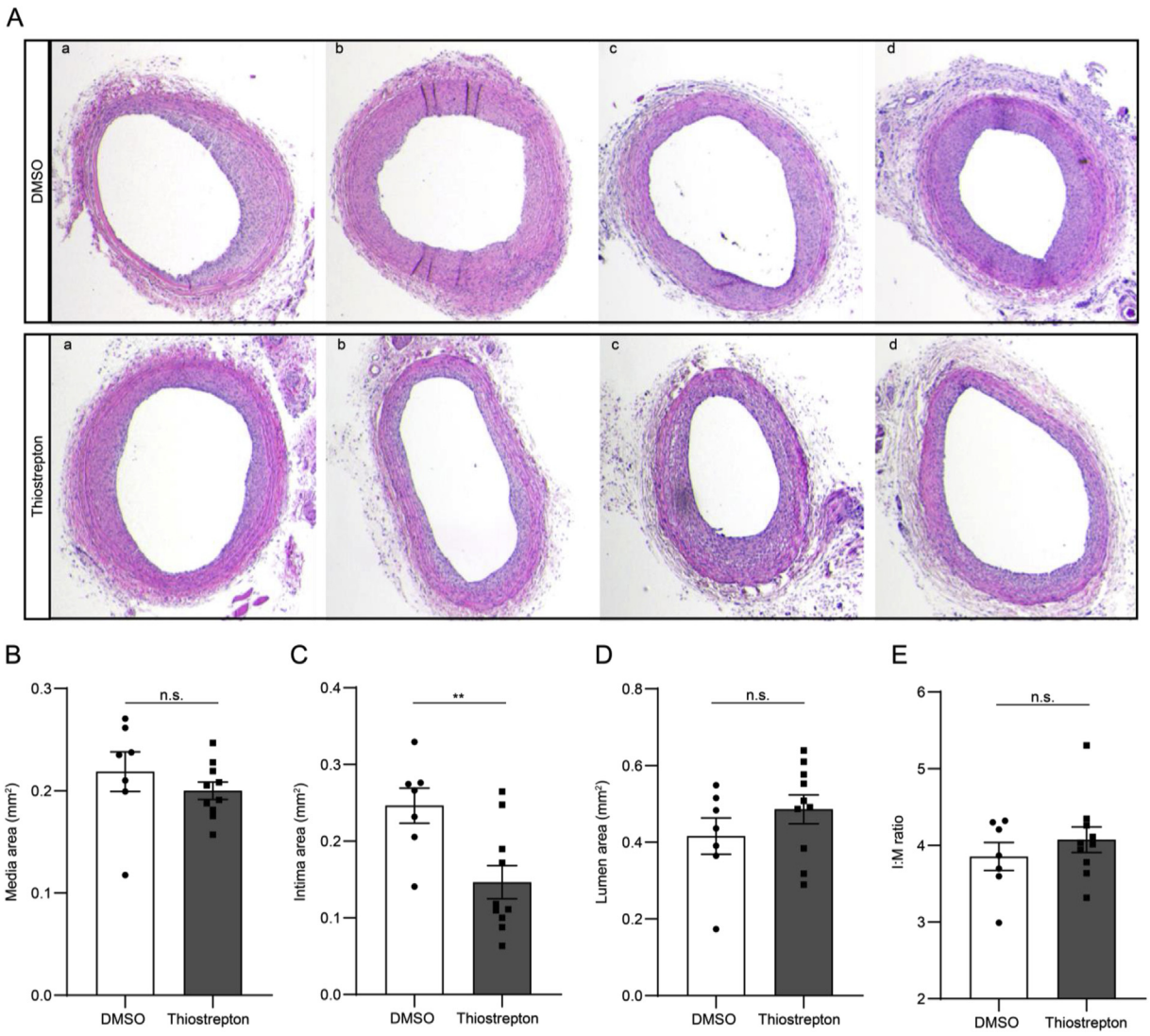

Figure 6. Thiostrepton mitigates intimal thickening following balloon injury. (A) Representative hematoxylin and eosin sections of injured arteries 14 days after balloon injury. Top panel shows 4 DMSO-treated rats (a, b, c, d) and bottom panel shows 4 thiostrepton-treated rats (a, b, c, d). Total number was 7 DMSO-treated and 10 thiostrepton-treated rats. Scale bars 200 μm. (B) Average media area for each treatment group (DMSO: n = 7) (thiostrepton: n = 10). P = 0.3384. (C) Average intima area for each treatment group. P = .0075. (D) Average lumen area for each treatment group. P = 0.2657. (E) Average intima to media ratio for each treatment group. P = 0.3938. n.s.: not significant.

downstream targets [58] and does not target other FOXM1 members [59]. However, this does not rule out the possibility that thiostrepton has off-target effects. It is possible that treatment with other FOXM1 inhibitors like FDI-6 will serve as better alternatives; however, to our knowledge, there are no known reports of using FDI-6 in vivo. Future studies will be required to assess the toxicity of FDI-6 and the bioavailability in animal models of restenosis. Rigorous efforts should be made to confirm the specificity of these FOXM1 inhibitors.

In conclusion, we have established a relation between FOXM1, the proliferation of SMCs, and the formation of intimal hyperplasia following balloon injury. The identification of FOXM1 in human atherosclerotic plaque suggests FOXM1 may also play a role in various vascular diseases. Our findings that thiostrepton reduces intimal thickening support the therapeutic potential of targeting FOXM1 in alleviating injury-induced IH.

Data statement

The data that support the findings of this study are available from the authors on reasonable request.

Declarations

Author contribution statement

S. Franco: Conceived and designed the experiments; Performed the experiments; Analyzed and interpreted the data; Wrote the paper.

B. Liu: Analyzed and interpreted the data; Contributed reagents, materials, analysis tools or data.

A. Stranz and F. Lumani: Performed the experiments; Analyzed and interpreted the data.

D. Stewart, V. Pilli, M. Chaudhary, and G. Urabe: Performed the experiments.

M. Kelly, D. Yamanouchi, K. Kent: Contributed reagents, materials, analysis tools or data.

Funding statement

B. Liu was supported by a National Institutes of Health grant (5R01HL122562-04). S. Franco was supported by grants from the National Institutes of Health (3R01HL122562-02S1 and 3R01HL088447-

07S1), Cellular and Molecular Pathology Training Program (NIH/NIGMS 5T32GM081061). M. Chaudhary, D. Stewart and M. Kelly were supported by the Vascular Surgery Research Training Program (NIH/NHLBI/T32HL110853).

Competing interest statement

The authors declare no conflict of interest.

Additional information

Supplementary content related to this article has been published online at https://doi.org/10.1016/j.heliyon.2020.e04028.

Acknowledgements

We thank Dr. Uma Wesley and Dr. Robert Demspey for their advice and assistance pertaining to human carotid plaque samples. We would like to thank the UW-Madison Department of Surgery Histology Core for use of its services. We would also like to thank the members of our laboratory for their helpful insights and discussions, Dr. Glen Leverson for his biostatistics expertise, and Dr. Zsuzsanna Fabry for allowing us to use her confocal microscope.

References

[1] W. Health Organization, Cardiovascular Diseases (Cvds), 2009. Http://www.Who.Int/mediacentre/factsheets. https://ci.nii.ac.jp/naid/10025942218/.
[2] Thomas L. Intracoronary stent restenosis. In: UpToDate, Windecker S. (Ed) and Saperia GM (Dep Ed). UpToDate, Waltham, MA (Accessed 10 July 2018).
[3] M.R. Alexander, G.K. Owens, Epigenetic control of smooth muscle cell differentiation and phenotypic switching in vascular development and disease, Annu. Rev. Physiol. 74 (2012) 13–40.
[4] M.J. Osgood, K.M. Hocking, I.V. Voskresensky, F.D. Li, P. Komalavilas, J. Cheung-Flynn, C.M. Brophy, Surgical vein graft preparation promotes cellular dysfunction, oxidative stress, and intimal hyperplasia in human saphenous vein, J. Vasc. Surg. 60 (2014) 202–211.
[5] V.J. Dzau, R.C. Braun-Dullaeus, D.G. Sedding, Vascular proliferation and atherosclerosis: new perspectives and therapeutic strategies, Nat. Med. 8 (2002) 1249–1256.
[6] R.C. Braun-Dullaeus, M.J. Mann, V.J. Dzau, Cell cycle progression: new therapeutic target for vascular proliferative disease, Circulation 98 (1998) 82–89. https://www.ncbi.nlm.nih.gov/pubmed/9665064.
[7] T.V. Kalin, V. Ustiyan, V.V. Kalinichenko, Multiple faces of FoxM1 transcription factor: lessons from transgenic mouse models, Cell Cycle 10 (2011) 396–405.
[8] E.W.-F. Lam, J.J. Brosens, A.R. Gomes, C.-Y. Koo, Forkhead box proteins: tuning forks for transcriptional harmony, Nat. Rev. Cancer 13 (2013) 482–495.
[9] I. Wierstra, J. Alves, FOXM1, a typical proliferation-associated transcription factor, Biol. Chem. 388 (2007) 1257–1274.
[10] X. Chen, G.A. Müller, M. Quaas, M. Fischer, N. Han, B. Stutchbury, A.D. Sharrocks, K. Engeland, The forkhead transcription factor FOXM1 controls cell cycle-dependent gene expression through an atypical chromatin binding mechanism, Mol. Cell Biol. 33 (2013) 227–236.
[11] S.S. Myatt, M. Kongsema, C.W.-Y. Man, D.J. Kelly, A.R. Gomes, P. Khongkow, U. Karunarathna, S. Zona, J.K. Langer, C.W. Dunsby, R.C. Coombes, P.M. French, J.J. Brosens, E.W.-F. Lam, SUMOylation inhibits FOXM1 activity and delays mitotic transition, Oncogene 33 (2014) 4316–4329.
[12] D.R. Wonsey, M.T. Follettie, Loss of the forkhead transcription factor FoxM1 causes centrosome amplification and mitotic catastrophe, Cancer Res. 65 (2005) 5181–5189.
[13] P. Khongkow, A.R. Gomes, C. Gong, E.P.S. Man, J.W.-H. Tsang, F. Zhao, L.J. Monteiro, R.C. Coombes, R.H. Medema, U.S. Khoo, E.W.-F. Lam, FOXM1 to regulate KIF20A in mitotic catastrophe and breast cancer paclitaxel resistance, Oncogene 35 (2016) 990–1002. Paclitaxel targets.
[14] T. Tajsic, N.W. Morrell, Smooth muscle cell hypertrophy, proliferation, migration and apoptosis in pulmonary hypertension, in: Comprehensive Physiology, 2010.
[15] Z. Dai, M.M. Zhu, Y. Peng, H. Jin, N. Machireddy, Z. Qian, X. Zhang, Y.-Y. Zhao, Endothelial and smooth muscle cell interaction via FoxM1 signaling mediates vascular remodeling and pulmonary hypertension, Am. J. Respir. Crit. Care Med. (2018).
[16] V. Ustiyan, I.-C. Wang, X. Ren, Y. Zhang, J. Snyder, Y. Xu, S.E. Wert, J.L. Lessard, T.V. Kalin, V.V. Kalinichenko, Forkhead box M1 transcriptional factor is required for smooth muscle cells during embryonic development of blood vessels and esophagus, Dev. Biol. 336 (2009) 266–279.
[17] P.A. Suwanabol, S.M. Seedial, F. Zhang, X. Shi, Y. Si, B. Liu, K.C. Kent, TGF-β and Smad3 modulate PI3K/Akt signaling pathway in vascular smooth muscle cells, Am. J. Physiol. Heart Circ. Physiol. 302 (2012). H2211–9.
[18] M.M. Clowes, C.M. Lynch, A.D. Miller, D.G. Miller, W.R. Osborne, A.W. Clowes, Long-term biological response of injured rat carotid artery seeded with smooth muscle cells expressing retrovirally introduced human genes, J. Clin. Invest. 93 (1994) 644–651.
[19] T.C. Humphrey, G. Brooks, Cell Cycle Control: Mechanisms and Protocols, Springer Science & Business Media, 2005.
[20] G.-B. Liao, X.-Z. Li, S. Zeng, C. Liu, S.-M. Yang, L. Yang, C.-J. Hu, J.-Y. Bai, Regulation of the master regulator FOXM1 in cancer, Cell Commun. Signal. 16 (2018) 57.
[21] Y. Togashi, J. Shirakawa, K. Orime, M. Kaji, E. Sakamoto, K. Tajima, H. Inoue, A. Nakamura, Y. Tochino, Y. Goshima, I. Shimomura, Y. Terauchi, β-Cell proliferation after a partial pancreatectomy is independent of IRS-2 in mice, Endocrinology 155 (2014) 1643–1652.
[22] H.J. Park, R.H. Costa, L.F. Lau, A.L. Tyner, P. Raychaudhuri, Anaphase-promoting complex/cyclosome-CDH1-mediated proteolysis of the forkhead box M1 transcription factor is critical for regulated entry into S phase, Mol. Cell Biol. 28 (2008) 5162–5171.
[23] N.S. Hegde, D.A. Sanders, R. Rodriguez, S. Balasubramanian, The transcription factor FOXM1 is a cellular target of the natural product thiostrepton, Nat. Chem. 3 (2011) 725–731.
[24] J.M.-M. Kwok, S.S. Myatt, C.M. Marson, R.C. Coombes, D. Constantinidou, E.W.-F. Lam, Thiostrepton selectively targets breast cancer cells through inhibition of forkhead box M1 expression, Mol. Cancer Therapeut. 7 (2008) 2022–2032.
[25] A.L. Gartel, Suppression of the oncogenic transcription factor foxm1 by proteasome inhibitors, Scientifica 2014 (2014) 596528.
[26] M.V. Gormally, T.S. Dexheimer, G. Marsico, D.A. Sanders, C. Lowe, D. Matak-Vinković, S. Michael, A. Jadhav, G. Rai, D.J. Maloney, A. Simeonov, S. Balasubramanian, Suppression of the FOXM1 transcriptional programme via novel small molecule inhibition, Nat. Commun. 5 (2014) 5165.
[27] C. Liu, T. Su, F. Li, L. Li, X. Qin, W. Pan, F. Feng, F. Chen, D. Liao, L. Chen, PI3K/Akt signaling transduction pathway is involved in rat vascular smooth muscle cell proliferation induced by apelin-13, Acta Biochim. Biophys. Sin. 42 (2010) 396–402.
[28] Y. Zhao, S.K. Biswas, P.H. McNulty, M. Kozak, J.Y. Jun, L. Segar, PDGF-induced vascular smooth muscle cell proliferation is associated with dysregulation of insulin receptor substrates, Am. J. Physiol. Cell Physiol. 300 (2011) C1375–C1385.
[29] H. Quasnichka, S.C. Slater, C.A. Beeching, M. Boehm, G.B. Sala-Newby, S.J. George, Regulation of smooth muscle cell proliferation by β-catenin/T-cell factor signaling involves modulation of cyclin D1 and p21 expression, Circ. Res. (2006).
[30] D.M. DiRenzo, M.A. Chaudhary, X. Shi, S.R. Franco, J. Zent, K. Wang, L.-W. Guo, K.C. Kent, A crosstalk between TGF-β/Smad3 and Wnt/β-catenin pathways promotes vascular smooth muscle cell proliferation, Cell. Signal. 28 (2016) 498–505.
[31] W. Korver, J. Roose, H. Clevers, The winged-helix transcription factor Trident is expressed in cycling cells, Nucleic Acids Res. 25 (1997) 1715–1719.
[32] C. Yang, H. Chen, L. Yu, L. Shan, L. Xie, J. Hu, T. Chen, Y. Tan, Inhibition of FOXM1 transcription factor suppresses cell proliferation and tumor growth of breast cancer, Cancer Gene Ther. 20 (2013) 117–124.
[33] J.-M. Wang, B.-H. Ju, C.-J. Pan, Y. Gu, M.-Q. Li, L. Sun, Y.-Y. Xu, L.-R. Yin, MiR- 214 inhibits cell migration, invasion and promotes the drug sensitivity in human cervical cancer by targeting FOXM1, Am. J. Transl. Res. 9 (2017) 3541–3557. https://www.ncbi.nlm.nih.gov/pubmed/28861147.
[34] S. Zona, L. Bella, M.J. Burton, G. Nestal de Moraes, E.W.-F. Lam, FOXM1: an emerging master regulator of DNA damage response and genotoxic agent resistance, Biochim. Biophys. Acta 1839 (2014) 1316–1322.
[35] B. Pandit, A.L. Gartel, FoxM1 knockdown sensitizes human cancer cells to proteasome inhibitor-induced apoptosis but not to autophagy, Cell Cycle 10 (2011) 3269–3273.
[36] J.R. Carr, H.J. Park, Z. Wang, M.M. Kiefer, P. Raychaudhuri, FoxM1 mediates resistance to herceptin and paclitaxel, Cancer Res. 70 (2010) 5054–5063.
[37] X. Yang, Y. Shi, J. Yan, H. Fan, Downregulation of FoxM1 inhibits cell growth and migration and invasion in bladder cancer cells, Am. J. Transl. Res. 10 (2018) 629–638. https://www.ncbi.nlm.nih.gov/pubmed/29511457.
[38] D. Gomez, G.K. Owens, Smooth muscle cell phenotypic switching in atherosclerosis, Cardiovasc. Res. 95 (2012) 156–164.
[39] D. Gomez, G.K. Owens, Reconciling smooth muscle cell oligoclonality and proliferative capacity in experimental atherosclerosis, Circ. Res. 119 (2016) 1262–1264.
[40] A. Bourgeois, C. Lambert, K. Habbout, B. Ranchoux, S. Paquet-Marceau, I. Trinh, S. Breuils-Bonnet, R. Paradis, V. Nadeau, R. Paulin, S. Provencher, S. Bonnet, O. Boucherat, FOXM1 promotes pulmonary artery smooth muscle cell expansion in pulmonary arterial hypertension, J. Mol. Med. 96 (2018) 223–235.
[41] T. Inoue, K. Node, Molecular basis of restenosis and novel issues of drug-eluting stents, Circ. J. 73 (2009) 615–621. https://www.ncbi.nlm.nih.gov/pubmed/19282604.
[42] Y.-Y. Zhao, X.-P. Gao, Y.D. Zhao, M.K. Mirza, R.S. Frey, V.V. Kalinichenko, I.-C. Wang, R.H. Costa, A.B. Malik, Endothelial cell-restricted disruption of FoxM1 impairs endothelial repair following LPS-induced vascular injury, J. Clin. Invest. 116 (2006) 2333–2343.
[43] L.R. Penke, J.M. Speth, V.L. Dommeti, E.S. White, I.L. Bergin, M. Peters-Golden, FOXM1 is a critical driver of lung fibroblast activation and fibrogenesis, J. Clin. Invest. 128 (2018) 2389–2405.
[44] X. Ren, Y. Zhang, J. Snyder, E.R. Cross, T.A. Shah, T.V. Kalin, V.V. Kalinichenko, Forkhead box M1 transcription factor is required for macrophage recruitment during liver repair, Mol. Cell Biol. 30 (2010) 5381–5393.
[45] O.J. Lehmann, J.C. Sowden, P. Carlsson, T. Jordan, S.S. Bhattacharya, Fox's in development and disease, Trends Genet. 19 (2003) 339–344.

[46] B.A. Benayoun, S. Caburet, R.A. Veitia, Forkhead transcription factors: key players in health and disease, Trends Genet. 27 (2011) 224–232.
[47] P. Carlsson, M. Mahlapuu, Forkhead transcription factors: key players in development and metabolism, Dev. Biol. 250 (2002) 1–23. https://www.ncbi.nlm.nih.gov/pubmed/12297093.
[48] M.G. Davies, P.O. Hagen, Pathobiology of intimal hyperplasia, Br. J. Surg. 81 (1994) 1254–1269.
[49] M.L. Major, R. Lepe, R.H. Costa, Forkhead box M1B transcriptional activity requires binding of Cdk-cyclin complexes for phosphorylation-dependent recruitment of p300/CBP coactivators, Mol. Cell Biol. 24 (2004) 2649–2661. https://www.ncbi.nlm.nih.gov/pubmed/15024056.
[50] A. Miyashita, S. Fukushima, S. Nakahara, J. Yamashita, A. Tokuzumi, J. Aoi, A. Ichihara, H. Kanemaru, M. Jinnin, H. Ihn, Investigation of FOXM1 as a potential new target for melanoma, PloS One 10 (2015), e0144241.
[51] H.J. Park, J.R. Carr, Z. Wang, V. Nogueira, N. Hay, A.L. Tyner, L.F. Lau, R.H. Costa, P. Raychaudhuri, FoxM1, a critical regulator of oxidative stress during oncogenesis, EMBO J. 28 (2009) 2908–2918.
[52] G. Yu, A. Zhou, J. Xue, C. Huang, X. Zhang, S.-H. Kang, W.-T. Chiu, C. Tan, K. Xie, J. Wang, S. Huang, FoxM1 promotes breast tumorigenesis by activating PDGF-A anrming a positive feedback loop with the PDGF/AKT signaling pathway, Oncotarget 6 (2015) 11281–11294.
[53] A. Bowman, R. Nusse, Location, location, location: FoxM1 mediates β-catenin nuclear translocation and promotes glioma tumorigenesis, Cancer Cell 20 (2011) 415–416.
[54] N. Zhang, P. Wei, A. Gong, W.-T. Chiu, H.-T. Lee, H. Colman, H. Huang, J. Xue, M. Liu, Y. Wang, R. Sawaya, K. Xie, W.K.A. Yung, R.H. Medema, X. He, S. Huang, FoxM1 promotes β-catenin nuclear localization and controls Wnt target-gene expression and glioma tumorigenesis, Cancer Cell 20 (2011) 427–442.
[55] Y. Chen, Y. Li, J. Xue, A. Gong, G. Yu, A. Zhou, K. Lin, S. Zhang, N. Zhang, C.J. Gottardi, S. Huang, Wnt-induced deubiquitination FoxM1 ensures nucleus β-catenin transactivation, EMBO J. 35 (2016) 668–684.
[56] A. Sengupta, M. Rahman, S. Mateo-Lozano, O.M. Tirado, V. Notario, The dual inhibitory effect of thiostrepton on FoxM1 and EWS/FLI1 provides a novel therapeutic option for Ewing's sarcoma, Int. J. Oncol. 43 (2013) 803–812. https://www.spandidos-publications.com.
[57] M. Wang, A.L. Gartel, Micelle-encapsulated thiostrepton as an effective nanomedicine for inhibiting tumor growth and for suppressing FOXM1 in human xenografts, Mol. Cancer Therapeut. 10 (2011) 2287–2297.
[58] A.L. Gartel, Thiostrepton, proteasome inhibitors and FOXM1, Cell Cycle 10 (2011) 4341–4342.
[59] U.G. Bhat, M. Halasi, A.L. Gartel, Thiazole antibiotics target FoxM1 and induce apoptosis in human cancer cells, PloS One 4 (2009), e5592.